Excited State Intramolecular Proton Transfer Reactions in 2-(2-Hydroxyphenyl)benzimidazole in Micellar Solutions

Somes Kumar Das, Ashish Bansal, and Sneh Kumar Dogra*

Department of Chemistry, I. I. T. Kanpur, Kanpur-208016, India

(Received July 8, 1996)

Spectral characteristics of 2-(2-hydroxyphenyl)benzimidazole (HPBI) have been studied in solutions containing different compositions of dioxane–water mixtures, aqueous sodium dodecyl sulfate (SDS), hexadecyltrimethylammonium bromide (HTAB), and Triton X-100 (TX-100). The correlation curve between the fluorescence band maxima ($\bar{\nu}_{fl}$) and the dielectric constant of dioxane–water solutions provides a better rule than the pure solvents to find the polarity at the binding site of the fluorophore in micelles. The effective dielectric constant at the binding sites of SDS, HTAB, and TX-100 are found to be 40, 20, and 20, respectively. The values of the binding constants of HPBI to these micelles conform to the above results. pK_a values for various proton transfer reactions were determined at different concentrations of SDS, HTAB, and TX-100, both in the ground and singlet states, and these are discussed.

The photophysics and photochemistry of 2-(2-hydroxyphenyl)benzimidazole (HPBI)[1—7] and related molecules[8—21] have been studied extensively. The reason is because these compounds show excited state intramolecular proton transfer (ESIPT) and thus act as efficient sources of tunable dye lasers, as materials for protecting agents against UV radiation damage, and as materials for storing information at the molecular level. Recently Douhal et al.[7] have shown that the large red shifted fluorescence tautomer band (ca. 450 nm) is due to the ground state species I of HPBI where the intramolecular hydrogen bonding is present in the S_0 state and the normal Stokes-shifted fluorescence band in polar/protic solvents is due to the open structure of HPBI II (Chart 1). Earlier studies[3] have shown that the fluorescence band maximum of the tautomer III and its fluorescence quantum yield (ϕ_{fl}) are quite sensitive to the solvents, whereas the normal fluorescence band does not show much solvent dependency. Thus it is possible that a phototautomer fluorescence band of HPBI can be used as a spectral 'ruler' to determine the polarity of macromolecular sites where the molecules may be located.

The main aims of this study are as follows: (i) Since the spectral characteristics of this molecule are very sensitive to the environment, we have drawn a correlation diagram between the $\bar{\nu}_{fl}$ and the dielectric constant, using different compositions of dioxane–water mixtures as solvent to determine the polarity at the binding site of the micelles. The reason is that these mixtures provide a wide range of polarity and hydrogen bonding properties. On the other hand, polar/aprotic mixture provide a wide range of polarity but no hydrogen bonding. Thus the former mixtures represent very closely the micellar environments, because the micelles do contain water molecules and are involved in hydrogen bonding. (ii) In general the fluorescence quantum yields of the fluorophores increase in micellar media. Since this molecule has been used as a potential tunable dye laser, the use of micellar media may increase the intensity of the laser. (iii) This molecule possesses multifunctional groups. The equilibrium constants for the various prototropic reactions in micellar medium have been determined and discussed. Since both the acidic and basic centers are close to each other, the prototropic equilibrium constants may provide a better picture of the micellar properties. The micelles used are sodium dodecyl sulfate (SDS), hexadecyltrimethylammonium bromide (HTAB) and Triton X-100 (TX-100).

Materials and Methods

HPBI was prepared by refluxing *o*-phenylenediamine with *o*-hydroxybenzoic acid in polyphosphoric acid medium, as suggested earlier.[22] HPBI was purified by repeated crystallization from ethanol, followed by vacuum sublimation. The purity of the compound was checked by noting its melting point, single spot on TLC, spectral characteristics in agreement with the literature data, and similar fluorescence spectra when excited with different excitation wavelengths in nonpolar solvents. Extra pure grade of HTAB was procured from BDH chemicals. It was washed with ether and crystallized twice from ethanol–acetone mixture in the ratio of 80 : 20 (v/v). SDS (Thomas–Baker) was purified from ethanol. TX-100 was obtained from Aldrich Chemical Co. and used as received. Analytical grade sodium hydroxide and sulfuric acid were used as received. Heptane, dioxane, acetonitrile, and methanol were further purified as suggested in the literature.[23] Triply distilled water was used to prepare all the aqueous solutions.

Instruments used to measure absorption data, fluorescence intensities, and lifetimes of the excited singlet state, preparations of the solutions, adjustments of their pH, procedure to correct the fluorescence spectra, and calculation of the fluorescence quantum yields are the same as described in our recent papers.[24—28]

Results and Discussion

Spectral Characteristics. 1. Dioxane–Water Mixtures. The spectral properties of HPBI in different

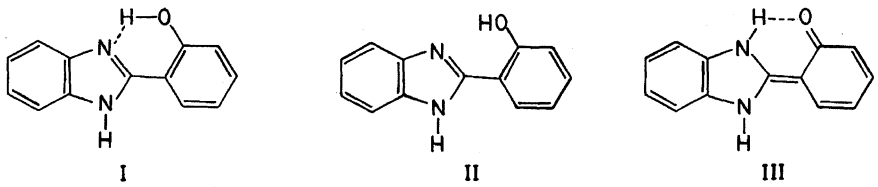

I II III

Chart 1.

compositions of dioxane–water solutions have been studied. $\bar{\nu}_{fl}$ (tautomer band), fluorescence intensity at one particular wavelength, Stokes shift, and band width at half the maximum height (BWHMH) have been plotted in Figs. 1a and 1b as a function of dielectric constant (ε) of different dioxane–water solutions. Sharp changes observed in these properties at the extreme compositions are due to the specific molecular interactions between HPBI and the solvent molecules. BWHMH is an exception; remains unchanged after 40% (v/v) of dioxane. This is because in protic solvents (such as methanol and water) the red edge excitation of HPBI gives rise to a band in the 400—425 nm range and has been assigned to the trace amounts of ionized form[7] (phenolate ion). At this concentration of water in dioxane ($\varepsilon \approx 25$), the ionized form of HPBI will be negligible, thus BWHMH remains constant, indicating only one kind of species, and emission occurs from a thermally relaxed state.

The red shift observed in λ_{max}^{fl} (430 nm band) with the addition of dioxane to water is due to the strengthening of the intramolecular hydrogen bond between the pyridinic nitrogen and the hydroxy proton, thus increasing the concentration of the phototautomer formed in the S_1 state. This is reflected by the plot in Fig. 1a. The other aspect observed in this plot is that the fluorescence intensity first increases, reaches a maximum (which is nearly double that observed in water and nearly 30% as large as that noticed in dioxane) at $55 \pm 5\%$ dioxane (v/v) in water and then decreases with increase of dioxane. The change in the fluorescence intensity at one particular wavelength cannot be used to find the nature of the environment around the fluorophore, as the fluorescence band is displaced largely toward red from polar/protic to nonpolar solvents. On the other hand, if one is interested in the wavelength of the tunable dye laser, one can attain it by using different compositions of dioxane–water mixtures. Further, instead of using either pure water or dioxane as solvents, use of 55% dioxane–water solution as solvent can be tried to achieve greater stimulated emission intensity.

The Stokes shift, in general, increases with increase in solvent polarity and hydrogen bonding capabilities.[29] But in our case the opposite trend was observed, as has already been explained. Thus it appears that, out of all the above-mentioned characteristics, variation of $\bar{\nu}_{fl}$ with the dielectric constant of the mixed solvents will prove to be useful to probe the micellar properties.

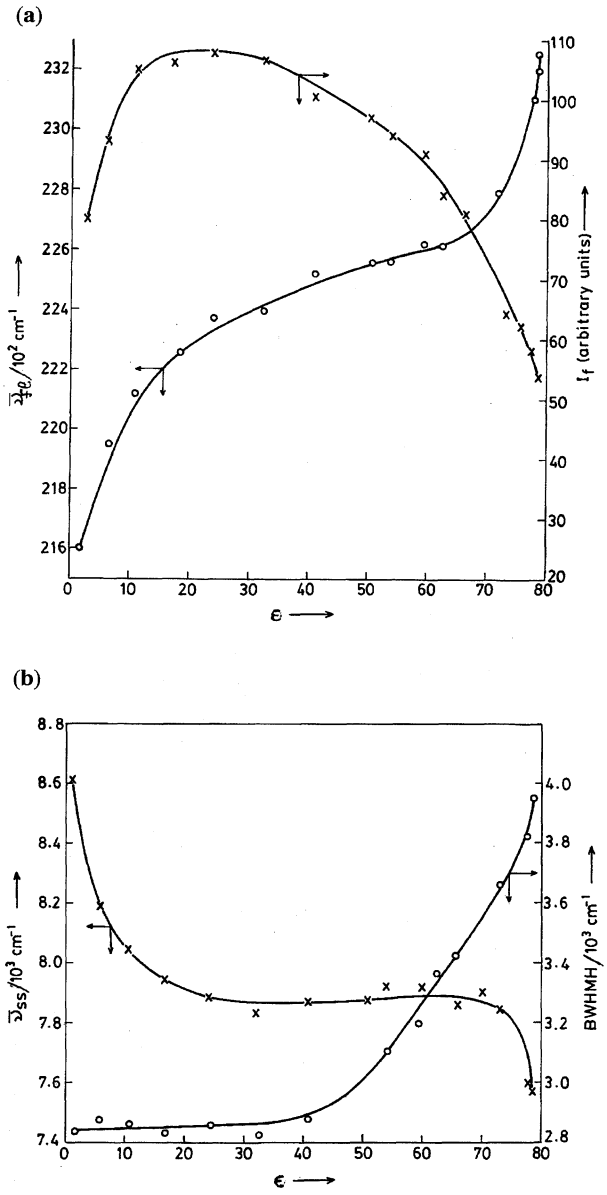

Fig. 1. (a) Plot of fluorescence intensity at band maxima and $\bar{\nu}_{max}^{fl}$ versus dielectric constant, [HPBI] = 1×10^{-5} M. (b) Plot of band width at half maximum height (BWHMH) and Stokes-shift versus dielectric constant, [HPBI] = 1×10^{-5} M.

2. Spectral Characteristics in Micelles. The spectral properties of HPBI have been studied in varying concentrations of SDS (pH = 8.7), HTAB (pH = 4.0), and TX-100 (pH = 7). The relevant data at surfactant concentration of 0.1 M (1 M = 1 mol dm^{-3}) have been compiled in Table 1. The fluorescence intensity measured at 443 nm band decreases in the beginning with the addition of SDS and HTAB, but it increases sharply as the surfactant concentration increased beyond the critical micelle concentration (cmc) and becomes nearly constant at 0.05 M SDS and 0.01 M HTAB. On the

Table 1. Absorption Band Maxima (λ_{ab}), Molar Extinction Coefficients (log ε_{max}), Fluorescence Band Maxima (λ_{fl}) and ϕ_{fl} of Neutral HPBI and Its Different Prototropic Species

	λ_{ab} (nm)				λ_{fl} (nm)					
Species	Aqueous	SDS	HTAB	TX-100	Aqueous		SDS		HTAB	TX-100
Neutral	325	329	333	333	350 (II)	430 (III)	354 (II)	442 (III)	449 (III)	450 (III)
pH=7.5	(4.23)	(4.36)	(4.38)	(4.40)	—	(0.33)	—	(0.45)	(0.75)	(0.63)
Monocation (IV) pH=1	330	337	—	334	364		380		—	—
Zwitterion (VI)	—	—	—	—	—	440	—	442	442	442
Monoanion(V)	345	394	353	353	411		413		418	413
pH=12	(4.31)	(4.33)	(4.33)	(4.4)	(0.62)	(0.63)			(0.68)	(0.64)

other hand, the fluorescence intensity of the tautomer band increases uniformly in TX-100. The 325 nm absorption band maximum is red-shifted by 4 to 8 nm, whereas the visible fluorescence band maximum is red-shifted by 12 to 20 nm and the shorter wavelength one is not shifted much in comparison to water. The fluorescence quantum yield of the visible band increases in all the surfactants and that of the UV band decreases marginally in SDS but vanishes in 0.01 M HTAB and TX-100. Further, the latter band is structured in SDS and structure can be explained by the vibrational frequency of 1400 ± 50 cm^{-1}, nearly the same as observed in less polar solvents[3] (1450 cm^{-1}). The absorption and fluorescence spectra of HPBI in different environments are shown in Figs. 2 and 3, respectively.

3. Effect of pH. The spectral characteristics of the monoanion (formed by the deprotonation of hydroxy group) were recorded at pH 12 for SDS and HTAB, and at pH 13 for TX-100. Unlike neutral species, the absorption and fluorescence band maxima of the monoanion in micelles are not different from those noticed in aqueous medium. The absorption spectrum of the monocation, formed by protonating the pyridinic nitrogen atom of HPBI is recorded at pH 4 in SDS and at pH 1 in TX-100, and this species is not formed

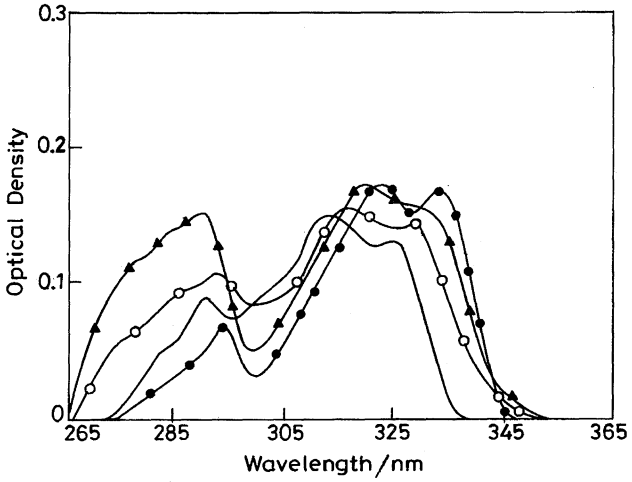

Fig. 2. Absorption spectrum of HPBI in different media, [HPBI] = 1×10^{-5} M, — water, ●—●—● HTAB, ▲—▲—▲ TX-100, ○—○—○ SDS.

even at pH 1 in HTAB. The fluorescence spectrum recorded by exciting at this pH gives rise to the zwitterion. The absorption band maximum of monocation is red-shifted by 4 to 7 nm, whereas the fluorescence spectrum of zwitterion is

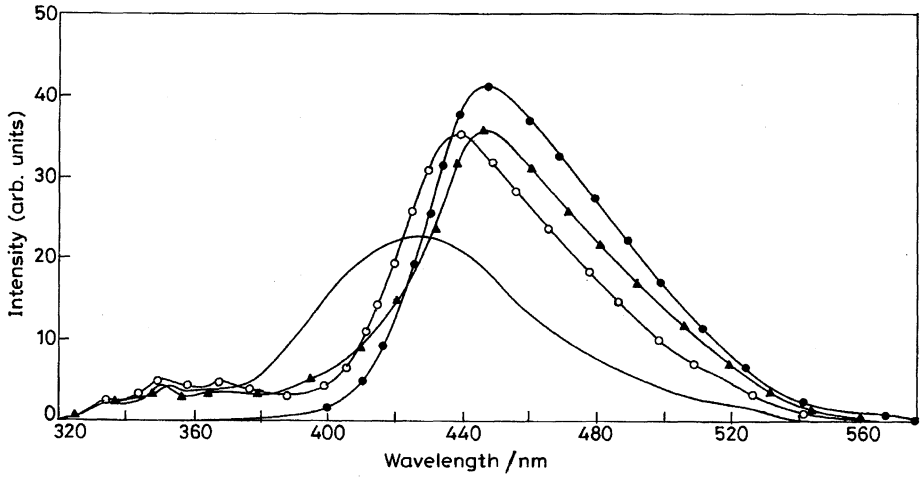

Fig. 3. Fluorescence spectrum of HPBI in different media, [HPBI] = 1×10^{-5} M, — water, ●—●—● HTAB, ▲—▲—▲ TX-100, ○—○—○ SDS.

red-shifted by 3 nm. In SDS the fluorescence spectrum of the monocation starts appearing below pH 3. The relevant data are compiled in Table 1.

4. Binding Constants and cmc. The binding constants of HPBI and its prototropic species have been determined using the equation suggested by Hirose and Sepulveda.[29] The values of K_s and cmc determined from the slope and the intercept are compiled in Table 2. The values of cmc obtained for all the three micelles at near neutral conditions agree with those obtained by other methods and reported in the literature.[30] The decrease in the cmc values of SDS and HTAB with the increase of ionic strength are consistent with the literature values.[29]

Data of Table 2 clearly indicate that for neutral HPBI the values of K_s are minimum for SDS and maximum for HTAB and TX-100. It is well known that the rate of intramolecular proton transfer in the S_1 state is very fast,[13,16] and it is complete in a few picoseconds even in rigid matrices at 4 K. The similarity in the values of K_s obtained using absorption and fluorescence data of both the bands lead us to the conclusion that the formation of the tautomer is also a very fast step in micellar medium and both the conformers II and III have nearly the same binding site in the micelles.

The value of binding constant of the monocation to SDS is higher than that of the neutral species; this is due to the presence of coulombic interactions with the oppositely charged polar head groups. The K_s value of the monocation of HPBI in TX-100 is calculated using only the absorption data because the monocation species present in the ground state, when excited, lead to the formation of zwitterions. The lower value of K_s determined using fluorescence data in comparison to that obtained using absorption data indicates this (Table 2).

5. Lifetimes in the Excited Singlet State. Lifetimes of the neutral HPBI were measured in heptane, dioxane, 55% (v/v) dioxane–water mixture, acetonitrile, methanol, water, 0.02 M SDS (pH 8.5), 0.01 M HTAB (pH 4), and 0.01 M TX-100 (pH 7) by exciting the solutions at 313 nm and measuring the decay at the fluorescence maxima. The decay curves followed a single exponential decay. The results along with ϕ_{fl} are compiled in Table 3. The agreement of τ_f with literature values is not bad,[5,7] whereas ϕ_{fl} in dioxane and methanol are slightly less and greater respectively than the reported ones.[7] The values of radiative (k_r) and nonradiative (k_{nr}) decay constants can be calculated from the following relations and are tabulated in Table 3.

Table 3. Fluorescence Quantum Yield, Lifetime (ns), k_r (10^8 s^{-1}) and k_{nr} (10^8 s^{-1}) in Different Environments

Medium	ϕ_{fl}	ϕ_{fl}[a]	τ_f	τ_f[a]	k_r	k_{nr}
Cyclohexane	0.50	0.55	3.9	3.6	1.3	1.2
Dioxane	0.51	0.65	4.2	4.2	1.2	1.18
Dioxane (55%)	0.79	—	4.5	—	1.75	0.47
Acetonitrile	0.66	0.72	4.3	4.1	1.5	0.8
Methanol	0.82	0.57	4.4	3.9	1.84	0.4
Water (pH 7)	0.33	—	3.0	—	1.1	2.23
SDS (0.01 M, pH 8.5)	0.45	—	3.7	—	1.2	1.51
HTAB (0.01 M, pH 4)	0.75	—	4.8	—	1.58	0.05
TX-100 (0.01 M, pH 7)	0.63	—	3.8	—	1.64	0.99

a) Ref. 7.

$$k_r = \phi_{fl}/\tau_f, \qquad k_{nr} = 1/\tau_f - k_r \tag{1}$$

The results clearly show that the values of nonradiative decay constants decrease with increase of polarity, but it is very large in water. The lifetime of the tautomer band in 0.01 M HTAB at pH 4 is greater than that obtained in all the solvents, suggesting that the nonradiative rate is very low in micelles.

6. Discussion. Photophysics of HPBI is very well studied in different solvents,[3,7] in methanol at different temperatures,[5] and at different acid-base concentrations.[3] It has been established that (i) the low energy absorption band is due to the presence of intramolecular hydrogen bonding, (ii) the large Stokes-shifted band is due to the tautomer III, and (iii) the normal Stokes-shifted band is due to open structure II. It has also been established that long wavelength absorption and fluorescence band maxima are blue-shifted with increase of polarity and proton donor/acceptor solvents. The short wavelength band is nearly absent in nonpolar (hydrocarbons) or weakly polar (ether) solvents. With the above discussion in mind, it can be qualitatively concluded that HPBI is transferred from more polar/protic to less polar/protic environments of the micelles.

Quantitatively, observation of single lifetime and the high value of K_s have established that at SDS concentration greater than 0.05 M and HTAB and TX-100 concentration greater than 0.01 M, HPBI is present at only one site in the micellar phase. A calibration curve was constructed by plotting emission maxima ($\bar{\nu}_{fl}$) versus dielectric constants of the polar/aprotic solvents. Based on this curve, the effective dielec-

Table 2. Binding Constants and cmc

Surfactant	Species	pH	K_s (M^{-1})	cmc[a] (M)	cmc[b]
SDS	Neutral	8.5	830	7.3×10^{-3}	6.8×10^{-3}
	Cation	1.0	1385	1.5×10^{-3}	—
HTAB	Neutral	6.5	3300	9.4×10^{-4}	8.4×10^{-4}
TX-100	Neutral	7.0	2800	2.2×10^{-4}	—
	Cation	1.0	3500[c] 450[d]	1.8×10^{-4}	—

a) From section Binding Constant and cmc. b) From the plot of fluorescence intensity vs. [D]. c) Absorption data. d) Fluorescence data.

tric constants of the binding site is close to 50 in each micelle, although the order is ε(SDS)>ε(HTAB)>ε(TX−100). This value is quite large, even if we assume that HPBI is located at the micellar interface.[31—33] On the other hand, the effective dielectric constants at the binding site of SDS, HTAB, and TX-100, obtained from the dioxane–water correlation diagram (Fig. 1a), are 40, 20, and 20, respectively, with much less water content. The low polarity and specific interactions at the binding site are also reflected when the tautomer band maxima in the micelles are compared with those noticed in glycol (ε=38, λ_{fl}=444 nm) and glycerol (ε=42, λ_{fl}=443 nm). Non-observation of 350 nm fluorescence band, higher values of τ_f, ϕ_{fl}, and K_s of HPBI in HTAB and TX-100 suggests that HPBI is located towards the core and away from the Stern layer, whereas in SDS HPBI is located in the Stern layer. HTAB and TX-100 reflect somewhat lower polarity and specific interactions than SDS. This is because the former two micelles possess a longer hydrocarbon chain than SDS; the flexibility of the longer chain may ease the movement of HPBI toward the core of micelles, leading to the lower polarity and low water content in HTAB and TX-100.[36] The similar results[24,26] that micelles are permeable to water are also observed from the I^- ion-induced fluorescence quenching.[34,35]

The decrease in the fluorescence intensity of HPBI with the addition of SDS and HTAB in the beginning is due to the interaction of monomers with the fluorophore, thus leading to premicellar aggregation. Similar behavior has also been observed in many other cases.[37—40] The concentration of SDS and HTAB at the premicellar aggregation is 2.5×10^{-3} and 3.5×10^{-4} M, respectively, whereas the cmc determined from the second inflection points is is 6.4×10^{-3} and 7.6×10^{-4} M for SDS and HTAB, respectively. The assignment of premicellar aggregation concentration to cmc value is a misnomer,[41] because this kind of behavior is present only in certain kinds of fluorophores and not always. The increase in the ϕ_{fl} of the phototautomer is due to the increase in the concentration of structure I in S_0 state and decrease in the collisional fluorescence quenching by the water molecules, as reflected in the lower rate of nonradiative decay process in micelles in comparison to water, consistent with similar behavior observed in the literature.[24]

Proton Transfer Reactions. 1. Ground State. The absorption spectra of various prototropic species of HPBI have been recorded in three micelles in the pH range of 1 to 13. The relevant data are compiled in Table 1, and the scheme depicting the different prototropic reactions is given below. It is clear that the proton transfer reactions of HPBI in S_0 state and in micellar medium are qualitatively similar to those in aqueous medium except for slight variations in acid-base concentration, i.e. monocation IV (pH<5 in SDS, pH<3 in TX-100, and pH<1 in HTAB); neutral I (pH range 8—5) and monoanion V (pH>13) (Chart 2). The spectral shifts observed on deprotonation or protonation are consistent with literature results.[42]

The apparent pK_a values in the ground state for various prototropic reactions were determined using absorption data, and these values are tabulated in Table 4. Apparent pK_a values for the monocation–neutral equilibrium increased in SDS micelles, decreased in TX-100 micelles, and cannot be determined in HTAB micelles. On the other hand, the apparent pK_a values for the neutral-monoanion equilibrium lowered in HTAB and increased in SDS and TX-100 with reference to those in aqueous medium.

Qualitatively the trends observed in the apparent pK_a values are consistent with Hartley's model,[43] but quantitatively

Table 4. Apparent pK_a for Different Prototropic Reactions

Equilibrium	[Dt]	pK_a		
		SDS	HTAB	TX-100
Monocation–Neutral	0.0	5.1	5.1	5.1
	0.005	5.65		
	0.01	6.7		
	0.02	6.8		3.1
	0.05	6.7		
Neutral–Monoanion	0.0	8.9	8.9	8.9
	0.0005	—	9.2	—
	0.001	—	8.25	—
	0.002	—	8.45	—
	0.005	—	8.52	—
	0.01	—	8.5	—
	0.02	9.8	8.6	11.2
	0.05	10.1	—	—
	0.1	10.4	—	—

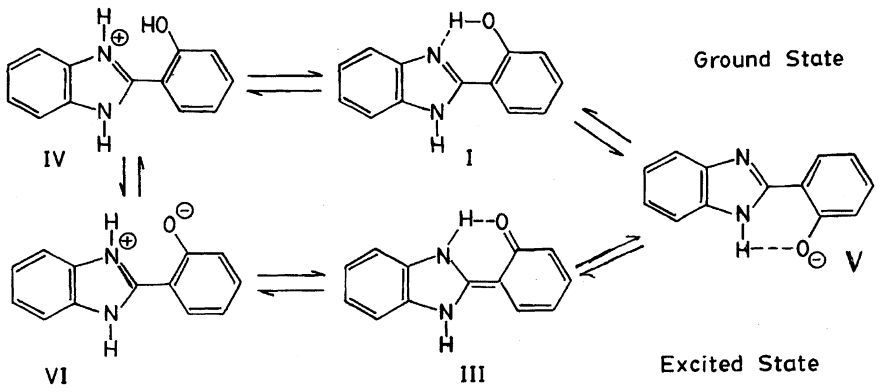

Chart 2.

a more refined model is needed. The results cannot be explained by the effective dielectric constant model at the site of prototropic reactions,[44—46] because of the lower dielectric constant in the micelles. This leads to the stabilization of the neutral species in comparison to ionic species. Thus the apparent pK_a value of monocation–neutral should be less and that of neutral–monoanion equilibrium should be more than those observed in aqueous medium. Our results in TX-100 are consistent with this model, whereas in ionic micelles the trends observed are the opposite and thus contradicts the predictions of the former model.

In the PIE model,[47—50] the changes in the pK_a values are due to the micellar medium effects and the distribution of the participating reactants between the bulk aqueous phase and much smaller micellar phase volume. Even though the lower dielectric constant at the binding site is unfavorable for the solubilization of ionic species of HPBI, the Coulombic interactions do favor the binding process. For this reason, effective concentration of neutral species and H^+ ions will be greater in SDS than in water, thus increasing pK_a for the monocation–neutral equilibrium and vice versa in HTAB. Similarly, a decrease in apparent pK_a values for the neutral–monoanion equilibrium in HTAB and an increase in SDS can be explained along the same lines. The validity of the PIE model was further verified by varying the surfactant concentrations. The data of Table 4 support the validity of this model.

2. Prototropic Reactions in Excited Singlet State. The fluorescence spectra of HPBI in all the three micelles have been recorded in the pH range of 1 to 13, and the data are compiled in Table 1. The behavior of the neutral–monoanion equilibrium in S_1 state is similar to that noticed in the S_0 state. The protonation reactions occurring in the S_1 state in all three micelles are similar to those occurring in water, but different from those taking place in the S_0 state. Based on the results in the aqueous system, the 380 nm band is assigned to monocation. Based on the following results, the 442 nm band in all the three micelles is assigned to the zwitterion: (i) Below pH 5.5 in SDS and at pH 1 in TX-100 more than 99% of the species in S_0 is present as monocations, which have open structures IV. It is well known[42] that the pyridinic nitrogen atom becomes a strong base and >NH, $-NH_2$, and –OH groups become a stronger acids in S_1 state. The latter feature is also established in the micellar system.[53] Considering this, it will be difficult for the proton to be dissociated from the pyridinic nitrogen atom of the monocation, followed by intramolecular hydrogen bonding and rearrangement to the tautomer structure III, whereas the proton can be dissociated from the –OH group in the S_1 state to form zwitterion. (ii) In case of 2-alkyl- and 2-aryl substituted benzimidazoles[52] as well as in 2-(2-methoxyphenyl) benzimidazole,[54] where the intramolecular hydrogen bonding is not possible, the protonation reaction occurring in the S_0 and S_1 states is exactly the same. (iii) The binding constant calculated for HPBI at pH 1 in TX-100, using absorption data (3500 M^{-1}) is different from that obtained from fluorescence data (450 M^{-1}), indicating that species present in S_0 and S_1 states are different. Unfortunately, a similar experiment was not successful in SDS because hardly any change is observed in the absorption spectrum of monocations and fluorescence spectrum of zwitterion, (iv) If 442 nm band is due to phototautomer III, the 355 nm band at pH less than 5 should also have been observed.

The pK_a^* values have been determined using fluorimetric titration method. These curves gave the ground state pK_a values, showing that neutral–monoanion equilibrium is not established in the S_1 state. This indicates that the lifetimes of these species are much shorter than the reciprocal of the protonation/deprotonation reactions. This behavior is similar to what is noticed in aqueous medium,[3] as well as in the reactions carried out in less polar medium.[55—57] The pK_a^* value for the zwitterion–tautomer equilibrium in TX-100 has been determined using tautomer fluorescence band, whereas in SDS it has been determined using 350 nm fluorescence band, because in SDS the fluorescence band maxima and the intensities of the zwitterion and the tautomer bands are similar. The values of pK_a^* so obtained from the fluorimetric titrations (2.9) are similar to the ground state pK_a values for the monocation–neutral equilibrium in micelles, but much less than those observed in the aqueous medium (6.5). This is consistent with the results that the pK_a values in S_0 and S_1 states are lowered in the less polar medium, e.g., the pK_a^* values for the above equilibrium in 21, 31, and 81% dioxane–water mixtures (v/v) are 4.95, 4.4, and 2.9, respectively, the same as the pK_a values of monocation–neutral equilibrium in the S_0 state. The pK_a^* for monocation–zwitterion equilibrium could not be determined because the formation of the latter species was either not complete at pH 1 in SDS or the monocation was not formed in HTAB and TX-100.

Conclusions

The effective dielectric constants at the binding site of HPBI in SDS, HTAB, and TX-100 are 40, 20, and 20, respectively. Binding constants, ϕ_{fl}, and τ_f of various species of HPBI to these micelles also confirm that HTAB and TX-100 provide a more hydrophobic environment for the probe than SDS. The fluorescence quantum yield of the phototautomer band is higher in 55% dioxane–water (v/v) mixture and micelles in comparison to that in water or dioxane as solvent. Changes in the pK_a values for monocation–neutral equilibrium in SDS and neutral–monoanion equilibrium in HTAB are due to smaller dielectric constant, surface potential, and the specific interactions of the indicator with ionic head groups of the micelles, whereas in TX-100 changes observed in the pK_a values are due only to the effective dielectric constant, Prototropic equilibria for various prototropic reactions are not established in S_1 state.

The authors are thankful to the Department of Science and Technology, New Delhi, for financial support project no. SP/SI/H-19/91.

References

1) D. L. Williams and A. Hellar, *J. Phys. Chem.*, **74**, 4473 (1970).
2) A. Graness and G. Graness, *Z. Phys. Chem. (Leipzig)*, **267**, 173 (1986).
3) H. K. Sinha and S. K. Dogra, *Chem. Phys.*, **102**, 337 (1986).
4) A. U. Acuna, F. Amat, J. Catalan, A. Costela, J. M. Figuera, and J. M. Munoz, *Chem. Phys. Lett.*, **132**, 567 (1986).
5) K. Das, N. Sarkar, D. Majumdar, and K. Bhattacharyya, *Chem. Phys. Lett.*, **198**, 443 (1992).
6) A. U. Acuna, F. Amat-Guerrie, F. Costela, A. Douhat, J. M. Figurera, F. Florido, and R. Sastre, *Chem. Phys. Lett.*, **187**, 198 (1991).
7) A. Douhel, F. Amat-Guerri, and A. U. Acuna, *J. Photochem. Photobiol. A*, **78**, 127 (1994), and references listed therein.
8) P. J. Thistlethewaite and P. J. Corkilt, *Chem. Phys. Lett.*, **85**, 317 (1982).
9) G. J. Woolfe, M. Meizing, S. Schneider, and F. Dorr, *Chem. Phys.*, **77**, 213 (1983).
10) R. S. Becker and W. F. Richy, *J. Am. Chem. Soc.*, **89**, 1298 (1967).
11) A. Mordzinksi and Z. Grabowaska, *Chem. Phys. Lett.*, **90**, 122 (1982).
12) N. P. Ernsting, *J. Phys. Chem.*, **89**, 4932 (1985).
13) P. F. Barbara, P. M. Rentzepies, and L. F. Brus, *J. Am. Chem. Soc.*, **102**, 2786 (1980).
14) F. Larmer, T. Elsasser, and W. Kaiser, *Chem. Phys. Lett.*, **148**, 119 (1988).
15) A. J. G. Strajdjord and P. F. Barbara, *J. Phys. Chem.*, **89**, 2355 and 2362 (1985).
16) P. F. Barbara, P. K. Walsh, and L. E. Brus, *J. Phys. Chem.*, **93**, 23 (1989).
17) M. Weichmann, H. Port, W. Frey, F. Larmer, and T. Elsasser, *J. Phys. Chem.*, **95**, 1918 (1991), and references listed therein.
18) G. A. Brucker, T. C. Swinney, and D. F. Kelley, *J. Phys. Chem.*, **95**, 3190 (1991).
19) T. C. Swinney and D. F. Kelley, *J. Phys. Chem.*, **95**, 1036 (1991).
20) M. Krishnamurthy and S. K. Dogra, *J. Photochem. Photobiol. A*, **32**, 235 (1986).
21) M. Itoh and Y. Fuziwara, *J. Am. Chem. Soc.*, **107**, 1561 (1985).
22) C. M. Orlando, J. G. Wirth, and D. R. Health, *J. Org. Chem.*, **35**, 3147 (1970).
23) J. A. Riddick and W. B. Bunger, in "Techniques of Chemistry," ed by A.W. Wiesseberger, Wiley Interscience, New York (1970), Vol. 8, Organic Solvents, pp. 592, 644, and 695.
24) R. S. Sarpal and S. K. Dogra, *J. Chem. Soc., Faraday Trans.*, **88**, 2725 (1992).
25) R. S. Sarpal and S. K. Dogra, *J. Photochem. Photobiol. A*, **69**, 329 (1993).
26) R. S. Sarpal and S. K. Dogra, *Indian J. Chem., Sect. A*, **32A**, 754 (1993).
27) J. K. Dey and S. K. Dogra, *J. Phys. Chem.*, **98**, 3638 (1994).
28) S. Nigam, R. S. Sarpal, and S. K. Dogra, *Z. Phys. Chem., Abt. A*, **186A**, 31 (1994).
29) C. Hirose and L. Sepulveda, *J. Phys. Chem.*, **85**, 3689 (1982).
30) P. Mukerjee and K. J. Mysels, in "Critical Micelle Concentration of Aqueous Surfactants System," NSRDS-NBS, Washington, D. C. (1971), Vol. 36.
31) K. Kano, Y. Yeno, and S. Hashimoto, *J. Phys. Chem.*, **89**, 3161 (1985).
32) K. Kalyanasundaram and J. K. Thomas, *J. Phys. Chem.*, **87**, 2176 (1977).
33) P. Mukerjee and J. R. Cardinal, *J. Phys. Chem.*, **82**, 1620 (1978).
34) E. Blatt and P. Ghiggino, *Biochim. Biophys. Acta*, **822**, 43 (1985), and references listed therein.
35) R. S. Sarpal and S. K. Dogra, *J. Photochem. Photobiol. A*, **88**, 147 (1995).
36) F. Grieser and C. J. Drummond, *J. Phys. Chem.*, **92**, 5580 (1988).
37) M. E. Diaz-Grecia and A. Suaz-Medal, *Talanta*, **33**, 255 (1985).
38) M. E. Skarydora and L.Cermakova, *Collect. Czech. Chem. Commun.*, **47**, 776 (1982).
39) K. M. Kali, E. L. Kussler, and D.F. Evans, *J. Phys. Chem.*, **85**, 593 (1980).
40) S. Nagam, R. S. Sarpal, and S. K. Dogra, *J. Colloid Int. Sci.*, **163**, 152 (1994).
41) S. Kundu and N. Chattopadhyay, *Chem. Phys. Lett.*, **228**, 79 (1994).
42) J. F. Ireland and P. A. H. Wyatt, *Adv. Phys. Org. Chem.*, **12**, 159 (1976).
43) G. S. Hartley, *Q. Rev., Chem. Soc.*, **2**, 152 (1948).
44) M. S. Fernandez and P. J. Fromherz, *J. Phys. Chem.*, **81**, 1955 (1977).
45) C. J. Drummond, F. Grieser, and T. W. Healy, *J. Phys. Chem.*, **92**, 2604 (1988).
46) C. J. Drummond, F. Grieser, and T. W. Healy, *J. Chem. Soc., Faraday Trans. 1*, **1988**, 521, 537, 551, and 561, and reference listed therein.
47) C. A. Bunton, L. S. Romsted, and L. Sepulveda, *J. Phys. Chem.*, **84**, 2611 (1980).
48) L. S. Romsted, *J. Phys. Chem.*, **89**, 5107 and 5113 (1985).
49) C. A. Bunton and G. Savier, *Adv. Phys. Org. Chem.*, **22**, 213 (1986).
50) L. S. Romsted and D. Zenette, *J. Phys. Chem.*, **92**, 4690 (1988), and the references sited therein.
51) U. Khuango, R. MacDonald, and B. K. Selinger, *Z. Phys. Chem. (Frankfurt) (NF)*, **101**, 209 (1987).
52) S. K. Saha, P. Tiwari, and S. K. Dogra, *J. Phys. Chem.*, **98**, 5933 (1994).
53) S. Nigam and S. K. Dogra, *J. Photochem. Photobiol. A*, **54**, 214 (1990).
54) S. K. Das and S. K. Dogra, unpublished results.
55) B. K. Selinger, *Aus. J. Chem.*, **30**, 2087 (1977).
56) B. K. Selinger and A. Weller, *Aus. J. Chem.*, **30**, 2377 (1977).
57) C. M. Harris and B. K. Selinger, *Z. Phys. Chem. (Wiesbaden)*, **134**, 65 (1983).